PCCP

PAPER

View Article Online
View Journal | View Issue

Cite this: *Phys. Chem. Chem. Phys.*, 2014, **16**, 14912

The bending machine: CO_2 activation and hydrogenation on δ-MoC(001) and β-Mo_2C(001) surfaces

Sergio Posada-Pérez,[a] Francesc Viñes,[a] Pedro J. Ramirez,[bc] Alba B. Vidal,[cd] José A. Rodriguez[c] and Francesc Illas*[a]

Received 5th May 2014,
Accepted 5th June 2014

DOI: 10.1039/c4cp01943a

www.rsc.org/pccp

The adsorption and activation of a CO_2 molecule on cubic δ-MoC(001) and orthorhombic β-Mo_2C(001) surfaces have been investigated by means of periodic density functional theory based calculations using the Perdew–Burke–Ernzerhof exchange–correlation functional and explicitly accounting for (or neglecting) the dispersive force term description as proposed by Grimme. The DFT results indicate that an orthorhombic β-Mo_2C(001) Mo-terminated polar surface provokes the spontaneous cleavage of a C–O bond in CO_2 and carbon monoxide formation, whereas on a β-Mo_2C(001) C-terminated polar surface or on a δ-MoC(001) nonpolar surface the CO_2 molecule is activated yet the C–O bond prevails. Experimental tests showed that Mo-terminated β-Mo_2C(001) easily adsorbs and decomposes the CO_2 molecule. This surface is an active catalyst for the hydrogenation of CO_2 to methanol and methane. Although MoC does not dissociate C–O bonds on its own, it binds CO_2 better than transition metal surfaces and is an active and selective catalyst for the $CO_2 + 3H_2 \rightarrow CH_3OH + H_2O$ reaction. Our theoretical and experimental results illustrate the tremendous impact that the carbon/metal ratio has on the chemical and catalytic properties of molybdenum carbides. This ratio must be taken into consideration when designing catalysts for the activation and conversion of CO_2.

Introduction

Carbon dioxide (CO_2) is the most abundant greenhouse gas in Earth's atmosphere owing mostly to vast emissions derived from human activities. In the last few years CO_2 chemistry has become a very attractive area of research, not only for environmental reasons, but also due to the potential use of CO_2 as an alternative and economical feedstock.[1–4] The recovery of CO_2 for its hydrogenation to alcohols or other hydrocarbon compounds is an important approach to recycle the released carbon dioxide.[4] However, for these reactions to occur, the chemical activation of the CO_2 molecule is a necessary and oftentimes crucial step, which typically implies charge transfer from the catalyst and the molecular bending.[5]

Most of the catalysts used in the industry for the above-mentioned reactions use metal nanoparticles such as Ni, Pd, or Pt as an active phase that are supported either on oxides or fine sulfides.[6] Due to their complexity and cost, experiments are typically performed using model supported nanoparticles.[7] In the current search for new catalysts,[8] Transition Metal Carbides (TMCs) have arisen as appealing alternatives, because they exhibit broad and amazing physical and chemical properties.[9] These may be viewed as the result of combined properties of covalent solids, ionic crystals, and transition metals.[10] Because of these properties and their low cost, TMCs have become a type of materials with an increasing role in heterogeneous catalysis in the last few decades, either using them as catalysts or as supports for metal nanoparticles. The pioneering work of Levy and Boudart indicated that tungsten carbide showed catalytic activity very similar to or even better than platinum, for a variety of reactions.[11] Since then, the number of reactions catalyzed by TMCs has greatly increased. Beyond the catalytic activity *per* se, another very important application that has been contemplated is the ability to use TMCs as supports for metal nanoparticles. For example, Rodriguez *et al.* have shown that Au and Cu nanoparticles supported on TiC(001) are excellent catalysts for the hydrogenation of olefins, the hydrodesulfurization of thiophene, and the adsorption and decomposition of SO_2.[12–16] Also, TiC(001) and Au–TiC(001) systems have been found to catalyze H_2 dissociation[17,18] and CO oxidation.[19] In the latter,

[a] *Departament de Química Física & Institut de Química Teòrica i Computacional (IQTCUB), Universitat de Barcelona, c/Martí i Franquès 1, 08028 Barcelona, Spain. E-mail: francesc.illas@ub.edu*
[b] *Facultad de Ciencias, Universidad Central de Venezuela, Apartado 20513, Caracas 1020-A, Venezuela*
[c] *Chemistry Department, Brookhaven National Laboratory, Bldg. 555, Upton, NY 11973, USA*
[d] *Centro de Química, Instituto Venezolano de Investigaciones Cientificas (IVIC), Apartado 21827, Caracas 1020-A, Venezuela*

the attachment strength of CO on the TiC(001) surface or Au clusters is not very different,[20] but O_2 adsorption energy is higher on the Au–TiC(001) system.

It should be borne in mind that titanium carbide is a cumbersome support to be used in applications due to the difficulty in obtaining nanoparticles under working conditions. It is therefore better to work with δ-MoC and β-Mo_2C because they are much more active and do not require special conditions for their synthesis. Molybdenum carbides have been used as catalysts in different reactions: The orthorhombic β-Mo_2C has been proposed as a possible substitute to the commercial Cu-based catalyst used to carry out the Water-Gas-Shift (WGS) reaction[21,22] and also as a highly beneficial support to Pt nanoparticles in the catalyzed WGS reaction.[23] Moreover, β-Mo_2C has been recently found to be not only a good support to Ni nanoparticles, but also an active phase to the so-called Ni/β-Mo_2C bifunctional catalyst used in the methane dry reforming process. The catalytic activity of these systems has been previously predicted based on Density Functional Theory (DFT) calculations[24,25] and, very recently, has become the focus of a detailed mechanistic study.[26] Furthermore, it has been predicted that δ-MoC(001) can easily dissociate molecular oxygen[27] and DFT calculations showed the very high catalytic power of hexagonal α-Mo_2C on ammonia dehydrogenation.[28] Also, hexagonal α-Mo_2C(001) and orthorhombic β-Mo_2C phases have been considered as catalysts for CO hydrogenation,[29–31] and very recently, β-Mo_2C(001) has been proposed for CO dissociation.[32]

The objective here is to explore and determine whether the CO_2 molecule adsorbs on the (001) surfaces of δ-MoC and β-Mo_2C and see if activation of CO_2 occurs, as a first, preliminary, and necessary step for using molybdenum carbides as catalysts in CO_2 chemistry. An important issue is to determine how the activity towards CO_2 activation changes with the carbon/metal ratio in the carbide. It will be shown that CO_2 gets activated on δ-MoC(001) and the C-terminated β-Mo_2C(001), whereas an almost barrierless dissociation occurs on Mo-terminated β-Mo_2C(001), pointing to these surfaces as ideal active phases of molybdenum carbide composites for CO_2 activation. Indeed, experimental tests show that Mo-terminated β-Mo_2C(001) easily adsorbs and decomposes the CO_2 molecule. It is shown that this surface is also an active catalyst for the hydrogenation of CO_2 to methanol and methane.

Computational and experimental methods

A. Computational details

Periodic density functional calculations were carried out using the Vienna Ab initio Simulation Package (VASP)[33] for the slab surface models depicted in Fig. 1. Exchange–correlation effects have been accounted for by means of the generalized gradient approximation using the Perdew–Burke–Ernzerhof (PBE) exchange–correlation (xc) functional,[34] given the suitability of such an xc functional for the description of bulk and surfaces of molybdenum carbide compounds.[35] The van der Waals (vdW) correction proposed by Grimme[36] has been used to test the difference between the uncorrected calculations and calculations with vdW correction. In these calculations the valence electron density is expanded in a plane-wave basis set and the effect caused by the core electrons on the valence region is described

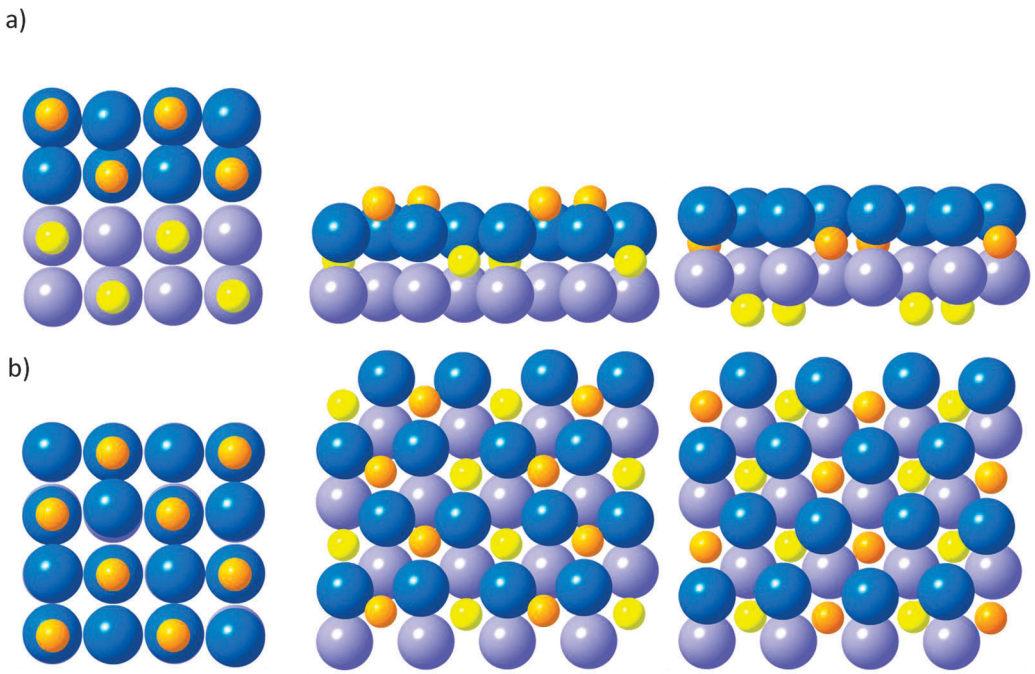

Fig. 1 Sketches of the studied surfaces: The δ-MoC(001) (left), β-Mo_2C(001)-C (middle), and β-Mo_2C(001)-Mo (right). Surfaces are shown by (a) side view and (b) top view. Blue and orange balls denote Mo and C atoms, respectively. The two layers that are relaxed colored darker.

by the projector augmented wave method of Blöchl[37] as implemented by Kresse and Joubert.[38] The kinetic energy cut-off for the plane wave basis set was set to 415 eV, proven to be enough to gain converged results for adsorbates on carbides in general, and in molybdenum carbides in particular.[35] The ionic relaxation convergence criterion was adjusted so that all forces acting on atoms were always smaller than 0.01 eV $Å^{-1}$. The electronic relaxation was considered converged when the total energy in subsequent iterations varied less than 10^{-5} eV. The slab models of the surface of interest contain four atomic layers, two of them previously relaxed, *i.e.* the (2 + 2) approach. In the case of cubic δ-MoC(001) this approach leads to a sufficiently thick slab as demonstrated in several previous studies.[27,39,40] However, in the case of the Mo-terminated β-Mo_2C(001) one may wonder if the smaller interlayer distance results in a more limited representation of the surface even if previous work on the properties of the naked surfaces strongly suggests that this choice is adequate.[35] To further confirm that this is the case for the predicted properties of adsorbed species, key calculations have been repeated with a slab model containing six atomic layers with the four topmost relaxed and the two bottom ones fixed as in the bulk. The calculated results with the 4 and 6 layer models exhibit very small variations as commented in the next section. For any of the studied surfaces a (2 × 2) supercell was employed. All supercells contain 32 atoms of Molybdenum. Cubic δ-MoC(001) also contains 32 Carbon atoms and orthorhombic β-Mo_2C contains 16 atoms of Carbon. The cell dimensions are 8.75 × 8.75 × 18.75 Å for δ-MoC(001) and 12.12 × 10.46 × 14.75 Å for β-Mo_2C (12.12 × 10.46 × 17.75 Å for the larger (4 + 2) slab model).[35] The vacuum space is superior to 10 Å in all cases.

CO_2 was adsorbed on one side of the slab, and during the course of the geometry optimization the CO_2 molecule as well as topmost two layers were fully relaxed. The reciprocal space was described by means of a 3 × 3 × 1 Monkhorst–Pack[41] scheme for the δ-MoC(001) nonpolar surface and a 5 × 5 × 1 grid for polar β-Mo_2C(001) surfaces. We show the different endings in Fig. 1. For β-Mo_2C(001) polar surfaces a counterdipole was placed in the middle of the vacuum region to avoid dipole coupling between repeated slabs. For δ-MoC(001) this correction is not necessarily included in the calculations because the variation of adsorption energy values (E_{ads}) is negligible (0.05 eV at most). The adsorption energy is calculated according to the following formula:

$$E_{ads} = E_{CO_2/Mo_nC} - (E_{Mo_nC} + E_{CO_2})$$

where E_{CO_2/Mo_nC} is the energy of CO_2 adsorbed on the corresponding surface; E_{Mo_nC} is the energy of the pristine surface; and E_{CO_2} is the energy of the isolated CO_2 molecule in an asymmetric box of 9 × 10 × 11 Å dimensions.

Note that on the β-Mo_2C(001) surface we have two possible terminations; the last layer can be composed of either C atoms or Mo atoms. We call β-Mo_2C(001)–C the surface with C termination atoms and β-Mo_2C(001)-Mo the one with Mo termination. Note in passing by that this polymorph exhibits an orthorhombic crystal structure, although some previous surface science studies often referred (incorrectly) to it as α-Mo_2C.

We explored all the adsorption sites of the CO_2 molecule on the commented surfaces, as shown in Fig. 2. We defined top sites where the adsorbate sits on top of surface atoms. This site is present in all the studied surfaces; for instance Top C is found in δ-MoC(001) surfaces and β-Mo_2C(001)–C and Top Mo in δ-MoC(001) and β-Mo_2C(001)-Mo surfaces. Note that in β-Mo_2C(001) there are two different Top sites. Bridge sites are considered when the contact is above the bond between two surface atoms and can involve either Mo–C, C–C, or Mo–Mo bonds; in 4-Hollow, the adsorbate binds simultaneously 4 surface atoms; finally, the regular Hollow sites imply a 3-fold coordination. These sites can be named according to the atoms the molecule is bonded to; for instance, MMC and MCC sites. The former indicates that the hollow site is formed by 2 surface Mo atoms and 1 surface C atom, whereas the latter implies 2 surface C atoms and 1 Mo atom. For Bridge, Hollow, and Top sites, in some cases, a superindex is added to differentiate among topologically distinct sites within the same cell. Finally, note that the CO_2 adsorption was tested on all possible sites, including different

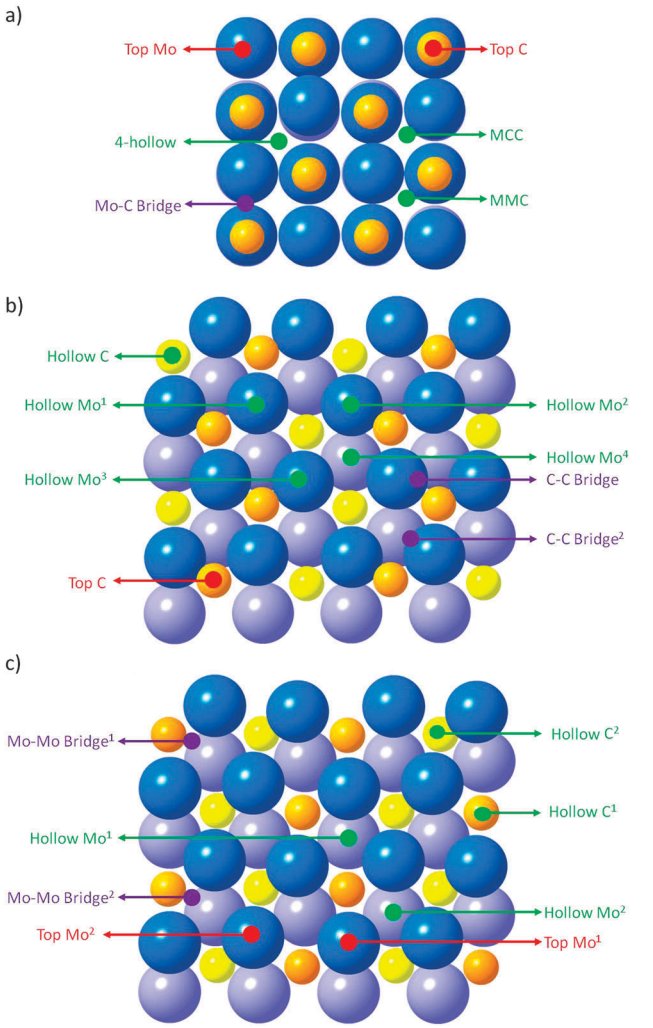

Fig. 2 Sketches of the different CO_2 adsorptions sites for the studied surfaces. The images indicate the top view of (a) δ-MoC(001), (b) β-Mo_2C(001)-C, and (c) β-Mo_2C(001)-Mo surfaces. Sphere coloring is as in Fig. 1.

coordination contacts through molecule C or O atoms. Final adsorption optimized structures have been characterized as minima in the potential energy surface *via* appropriate frequency analysis. This was carried out using the Hessian matrix constructed from finite differences of analytical gradients with individual displacements of 0.03 Å in each cell direction and including both molecule atoms and those of the first layer of the carbide in the calculations. Diagonalization of the Hessian matrix thus obtained leads to positive eigenvalues only.

B. Experimental details

Experiments were carried out to investigate the adsorption and hydrogenation of CO_2 on polycrystalline MoC and on a Mo-terminated $Mo_2C(001)$ surface.[42] Ion bombardment and subsequent annealing at 1000 K were used to clean and prepare the $Mo_2C(001)$ surface.[43] Images of scanning tunneling microscopy indicate that under these conditions this surface has the expected bulk-terminated (1×1) orthorhombic periodicity,[43] with two or three rotationally misaligned orthorhombic domains. The surface of MoC examined in this study is best described as polycrystalline.[42] Surface impurities were removed by Ar^+ sputtering, and a C/Mo ratio close to 1 was restored by exposing this surface to C_2H_2 or C_2H_4 at 800–900 K.[42] Several attempts were made to prepare well-defined surfaces of δ-MoC oriented along the (001) plane of this carbide. However, it was not possible to prepare an ideal δ-MoC(001) surface. The preparation of this particular surface is very difficult due to the complex phase diagram of MoC.[44]

The experimental data were collected in a set-up that combined an ultra-high vacuum (UHV) chamber for surface characterization and a micro-reactor for catalytic tests.[45] The UHV chamber was equipped with instrumentation for X-ray photoelectron spectroscopy (XPS), low-energy electron diffraction (LEED), ion-scattering spectroscopy (ISS), and thermal-desorption mass spectroscopy (TDS).[45] In the studies of CO_2 hydrogenation, the sample was transferred to the reactor at ~300 K, then the reactant gases, 0.049 MPa (0.5 atm) of CO_2 and 0.441 MPa (4.5 atm) of H_2, were introduced and the sample was rapidly heated to the reaction temperature (500, 525, 550, 575, and 600 K). Product yields were analyzed by a gas chromatograph.[46,47] In our experiments data were collected at intervals of 15 min up to a total reaction time of 270 min. The amount of molecules (CO, CH_4, or CH_3OH) produced in the catalytic tests was normalized by the active area exposed by the sample and the total reaction time. The kinetic experiments were done in the limit of low conversion (<5%).

Results

A. Theoretical studies

First of all we determined the CO_2 molecule orientation upon adsorption. To this end different starting structures were considered. In the perpendicular to surface orientation, one oxygen interacts with the studied surfaces whereas in the parallel to surface orientation all CO_2 atoms are in contact with the surface. The calculations indicate that the parallel adsorption of CO_2 is much more favorable than the perpendicular adsorption by at least 0.5 eV. Consequently, in the following, only the results for parallel adsorption are discussed.

All adsorption sites on the δ-MoC(001) surface were studied and the results are summarized in Table 1. It is shown that the CO_2 molecule can adsorb in two competitive sites (see Fig. 3). In the first one, the C atom is above the MMC site and O atoms are on top of Mo surface atoms resulting in an adsorption energy value of −0.82 eV; in addition, upon adsorption the molecule forms one regular C–C bond (1.46 Å) with the surface C. In the second case, the C atom is on top of a surface C atom and O atoms bridge C–Mo surface bonds; the corresponding E_{ads} is −0.74 eV and the adsorbed molecule also forms a regular C–C bond (1.47 Å) with the surface C atom. In both cases the chemisorption of CO_2 leads to elongation of the C–O bonds from 1.17 Å as in vacuum calculations to 1.29 Å in the adsorbed molecule, highlighting the molecular activation. Note that the C–C bond length lies between a single and a double bond. Last but not least, the adsorption is accompanied by bending of the molecular angle reaching values in the 120–130° range. These structural changes are in perfect agreement with substrate → molecule charge transfer, which reduces the CO_2 bond order, although the bending can be viewed as well as a change in sp → sp^2 hybridization forced by the C–C bond formation. From the vdW values listed in Table 1 one sees that the geometries of these systems do not vary, and only adsorption strengths are increased, revealing that dispersive forces do not play a role in CO_2 activation. Although the preferential site for PBE and PBE-vdW is different,

Table 1 Results of CO_2 adsorption in molybdenum carbide surfaces

Surface	Functional	Site	E_{ads}/eV	d(C–C)/Å	d(C–O)/Å	α(OCO)/°	$\Delta Q(CO_2)$/a.u.
δ-MoC(001)	PBE	MMC	−0.82	1.46	1.30	122	−0.93
	PBE-vdW	MMC	−1.33	1.46	1.30	121	−1.02
	PBE	Top C	−0.74	1.47	1.29	129	−0.76
	PBE-vdW	Top C	−1.35	1.47	1.29	129	−0.93
β-Mo_2C(001)-C	PBE	Top C	−0.61	1.47	1.21/1.42	122	−0.76
	PBE-vdW	Top C	−1.02	1.47	1.21/1.42	122	−0.75
β-Mo_2C(001)-Mo	PBE	Top Mo	−3.27	—	1.22[a]	—	−0.91[b]/−1.95[c]
	PBE-vdW	Top Mo	−3.69	—	1.26[a]	—	−0.91[b]/−1.97[c]
	PBE	Bridge Mo	−1.38	—	1.27	133	−1.26
	PBE-vdW	Bridge Mo	−1.76	—	1.27	133	−1.27

[a] This distance belongs to the CO molecule adsorbed on the β-Mo_2C(001)-Mo surface. [b] This ΔQ is for the CO moiety. [c] This ΔQ is for the O moiety.

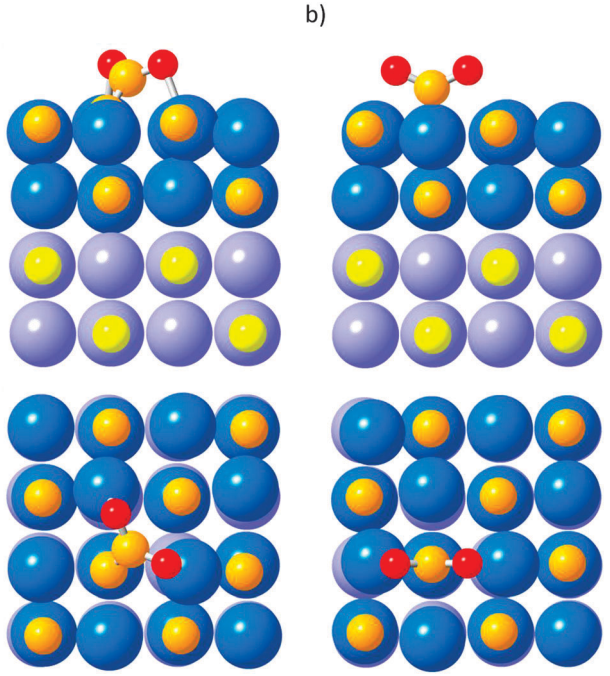

Fig. 3 Sketches of CO_2 adsorption on δ-MoC(001). For (a) MMC site and (b) Top C site. Surfaces are shown by the side view (top) and top view (bottom). Sphere coloring is as in Fig. 1.

one can still assure that the CO_2 adsorption on δ-MoC(001) presents two competitive adsorption sites.

In previous studies examining the interaction of CO and CO_2 on TiC(001)[20,45] it was found that adsorption resulted in the formation of a new C–C bond between the surface and the adsorbate. For adsorbed CO, the C–C bond length was found to be 1.33 Å, whereas in the CO_2–TiC(001) system and in the present CO_2–δ-MoC(001) systems the C–C bond distance is sensibly larger. The bending of the CO_2 molecule on TiC(001) was found to be indicative of a net carbide→CO_2 charge transfer.[48] For the present studied systems the charge distribution is estimated by the method of Bader,[49] and the results are shown in Table 1. By analyzing these results one observes that for the activation of CO_2 on δ-MoC(001) there is also a net carbide→CO_2 charge transfer of ~1 electron. In CO_2/TiC(001) the elongation of the C–O bonds is the same as that in the CO_2/δ-MoC(001) adsorption system. On the other hand, the adsorption energy of CO_2/TiC(001) is −0.62 eV, so the CO_2 molecule adsorbs sensibly stronger on the δ-MoC(001) surface. Thus, the longer C–C bond length in δ-MoC can be easily attributed to the size of Mo atoms compared to Ti atoms in TiC, and the concomitant increased steric repulsion. As we will discuss below, the differences in the strength of the CO_2–carbide binding when going from TiC to MoC probably help to make MoC a better catalyst for CO_2 hydrogenation than TiC.

The experimental results included later on are for Mo-terminated β-Mo_2C(001) but it is relevant to study the corresponding C-terminated surface as well. Hence, in a subsequent step, we investigated the interaction of CO_2 with these two β-Mo_2C(001) polar surfaces. The results (Table 1) show that the adsorption energy is −0.61 eV for β-Mo_2C(001)–C, this value being sensibly lower than that corresponding to the adsorption on the δ-MoC(001) surface. However, the C–C bond distance is still 1.47 Å and the C–O bond lengths are 1.21 and 1.42 Å, as on δ-MoC(001), the molecule gets activated, displaying an angle of 122°; the charge on CO_2 indicates that the β-Mo_2C(001)–C cedes ~0.75 electrons, irrespective of including or not the vdW correction. Initially, CO_2 was placed on top of a carbon surface, but during the optimization process displacement of the surface carbon atom bonded to the CO_2 molecule was observed. The final geometry is shown in Fig. 4. Here, the CO_2 molecule is adsorbed

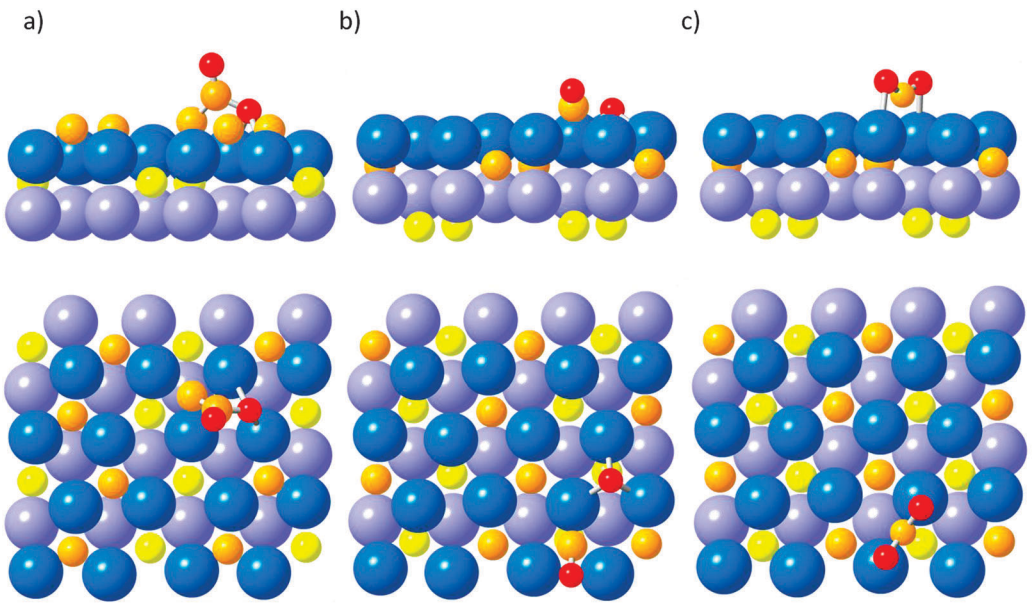

Fig. 4 Sketches of CO_2 adsorption on (a) β-Mo_2C(001)-C, (b) β-Mo_2C(001)-Mo with CO_2 dissociated, and (c) β-Mo_2C(001)-Mo with activated CO_2, showing the side view (top) and top view (bottom). Sphere coloring is as in Fig. 1.

with one C–C bond and one O bridging two Mo atoms. In this case preferential activation of a single C–O bond is observed. This fact can lead to an easier C–O bond cleavage and, therefore, to the dissociation of the adsorbed molecule (CO_2* → CO* + O*). In this surface, and the Mo-terminated one (see below), the vdW correction again does not significantly change the geometry of the adsorbed CO_2 molecule on β-Mo_2C(001) surfaces, yet the adsorption energies slightly increase. Despite the changes in the values of adsorption energy, all calculations indicate that the CO_2 adsorption on β-Mo_2C(001)–C is less favorable than on the other studied Molybdenum carbide surfaces, regardless of using the vdW correction.

As far as the β-Mo_2C(001)-Mo termination is concerned, interestingly, the placement of CO_2 on a Top Mo site of the surface results in an easy C–O bond cleavage with an adsorption energy of −3.27 eV and the final structure is depicted in Fig. 4, in which partial dissociation occurred. Different situations are possible for the orientation of the tilted adsorbed molecule although the energy differences between them are roughly ∼0.1 eV. It is also worth pointing out that the use of a thicker slab model containing 6 atomic layers leads to a slightly larger value of the adsorption energy (−3.43 eV) indicating that the influence of the surface model, even if noticeable, does not change any of the conclusions extracted from the present study. Note also that the quite large (>3 eV) absolute value of E_{ads} comes from considering the CO_2 molecule under vacuum as the energy reference; that is, the value adds the adsorption energy of CO and O moieties on the surface, but also considering the endothermicity of the C–O bond cleavage of CO_2. However, when the initial position is not on Top Mo, the CO_2 molecule gets activated, solely, and the surface is not able to break the C–O bond. The E_{ads} of the latter is −1.38 eV, and the molecule displays a C–O bond lengthening, reaching final values of 1.27 Å. Again, the CO_2 molecule receives charge density from the Molybdenum carbide substrate of ∼1.26 electron, and the molecule adopts a bended conformation with a molecular angle of 133°. As happened in the previous cases, the inclusion of vdW description does not significantly alter the final structure.

Here one may wonder whether this dissociation is realistic or an artifact of the optimization procedure. To further verify that this is indeed the physically meaningful dissociation pathway, a CO_2 adsorption energy profile has been constructed in a stepwise fashion optimizing points where the height of the C atom of the molecule was kept fixed and the transition state (TS) structure found from appropriate refinement of the energy maximum structure in the potential energy section in Fig. 5, followed by a characterization by frequency analysis, as carried out for the adsorption minima. The Hessian matrix displays only one negative eigenvalue corresponding to the imaginary frequency of the dissociation mode. It can be observed that at a distance of 2.75 Å a minimum energy is found with an adsorption energy of ∼0.2 eV, *i.e.* corresponding to a physisorption situation whereas at higher distances the CO_2 molecule does not feel the surface. The TS structure obtained involves a distance from the C atom to the surface of 2.30 Å, displaying C–O distances of 1.22–1.23 Å, significantly larger than the 1.17 Å C–O distance for the gas phase molecule, an O–C–O angle of 145° and involves an energy barrier of 0.76 eV. This energy barrier is larger than the physisorption energy but small enough so that it can be overcome at high coverage under realistic reaction conditions (see next section). Once the energy barrier is overcome, the reaction proceeds through a downhill path associated with a C–O bond cleavage reaching a minimum with a C-surface distance of 1.35 Å. It is worth stressing that such low activation barrier dissociations are not seldom, and have been previously observed for SO_2 dissociation on β-Mo_2C(001).[15] The Bader analysis shows that the CO moiety has gained ∼1 electron, so it can be considered as a carbonyl anion (CO^-), whereas the O moiety

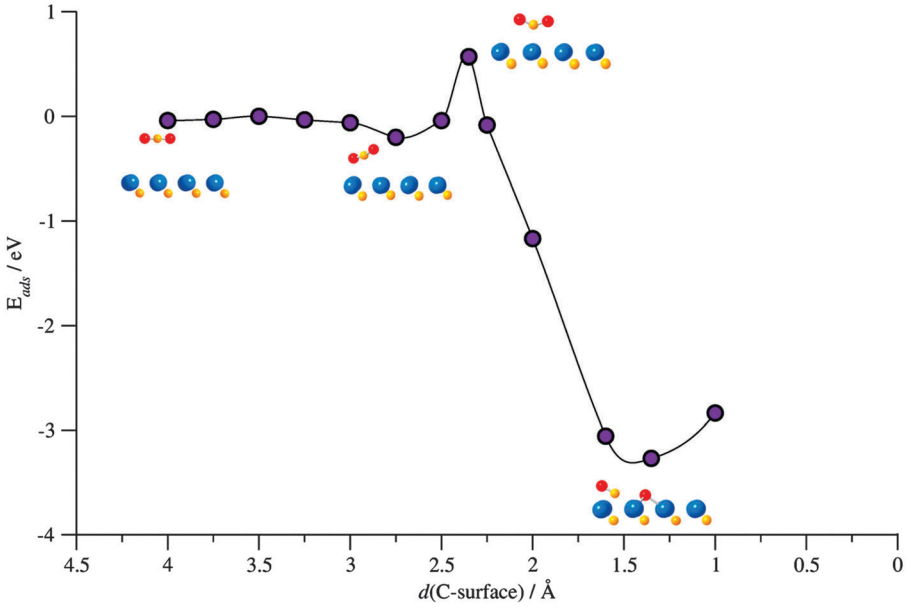

Fig. 5 CO_2 adsorption profile on β-Mo_2C(001)-Mo. Sketches of energy minima and some intermediate steps are shown.

has gained ~2 electrons, indicating that this moiety can be considered an oxygen anion (O^{2-}). Note that the structure of the CO moiety matches that of a recent similar study considering the CO adsorption and dissociation on β-Mo_2C(001)-Mo, studied using DFT at the PBE level.[32]

In the latter study the dissociation of CO was found to be exothermic, yet overcoming an energy barrier of more than 1 eV. This goes for a range of low temperatures in which CO_2 can be dissociated, yet the formed CO molecules can be stable at the surface. As we will see in the experiments described below, CO_2 does dissociate on the β-Mo_2C(001)-Mo surface to yield O and CO which could undergo further decomposition. The CO and C produced by the partial and total decomposition of CO_2 can be catalytically hydrogenated to form methanol and methane. Note that in a CO_2–β-Mo_2C(001)-Mo system, and according to the energy profile depicted in Fig. 5, the molecules will reach a physisorbed state, from which a fraction can be desorbed and the other can overcome a rather small dissociation energy barrier to reach the stationary point where CO and O moieties are present at the β-Mo_2C(001)-Mo surface.

B. Experimental studies

The O 1s region in XPS was used to investigate the adsorption of CO_2 on polycrystalline MoC and on a β-Mo_2C(001)-Mo surface at 300 K. The interaction of CO_2 with polycrystalline MoC was weak and a very small and broad peak was seen by XPS at O 1s binding energies between 531 and 533 eV. This binding energy can be attributed to the presence of CO or CO_2 species on the surface.[50] Since no signal was seen in the binding energy range of 528–530 eV where surface atomic O is expected,[51] it is likely that the weak features seen at 531–533 eV correspond to adsorbed CO_2. Since our MoC surface is probably rich in carbon, a direct comparison with the theoretical results for the well-defined δ-MoC(001) surface is not possible. For the adsorption of CO_2 on the β-Mo_2C(001)-Mo surface, XPS showed two separate features in the O 1s region. The first one peaked at 529.8–530.2 can be attributed to atomic oxygen.[51] The second one exhibited its maximum intensity at 531.2–531.5 eV and corresponds to adsorbed CO.[51] This implies that the $CO_2 \rightarrow CO + O$ reaction easily occurs on β-Mo_2C(001)-Mo. Fig. 6 compares the growth of the O 1s signal on MoC and β-Mo_2C(001)-Mo after several doses of CO_2. The data clearly indicate that β-Mo_2C(001)-Mo is much more reactive than MoC, in agreement with the trend seen in the theoretical results reported in Table 1.

Fig. 7 displays the uptake of CO and O on β-Mo_2C(001)-Mo after several doses of CO_2 at 300 K. The amount of O present on the surface is always larger than that of CO. Since CO binds well to similar surfaces of Mo_2C,[51] our results imply that two decomposition reactions are taking place on the carbide surface: $CO_2 \rightarrow CO + O$; $CO \rightarrow C + O$. This is particularly the case at low coverages when the concentration of O is more than double the concentration of CO. Once the adsorbate coverage increases on the surface, the full decomposition of CO_2 becomes more difficult and the ratio of surface O/CO decreases.

In the area of green chemistry, the activation of CO_2 and its hydrogenation to alcohols or other hydrocarbon compounds is an important approach to recycle carbon dioxide.[4] We found a correlation between the reactivity of the molybdenum carbides towards CO_2 and their catalytic activity. Fig. 8 compares the rates for methanol formation on MoC and β-Mo_2C(001)-Mo at 500 and 600 K. At 500 K, the rate for methanol formation on β-Mo_2C(001)-Mo is ~7 times larger than the rate on MoC. On the β-Mo_2C(001)-Mo surface, the $CO_2 \rightarrow CO + O$ reaction occurs spontaneously and the formed CO can be directly hydrogenated to form methanol. On the other hand, the cleavage of one C–O bond of CO_2 on MoC probably requires hydrogenation of the CO_2 molecule to form a HOCO intermediate that eventually decomposes producing a CO molecule which upon reaction with hydrogen forms methanol.[52] This sequence of steps is not fast at 500 K and MoC cannot compete with β-Mo_2C(001)-Mo as a catalyst for methanol synthesis. However, the high reactivity of β-Mo_2C(001)-Mo towards CO[32,51] can be problematic at very high temperatures. In Fig. 8, the rate for methanol production on β-Mo_2C(001)-Mo at 600 K is somewhat smaller than that at 500 K.

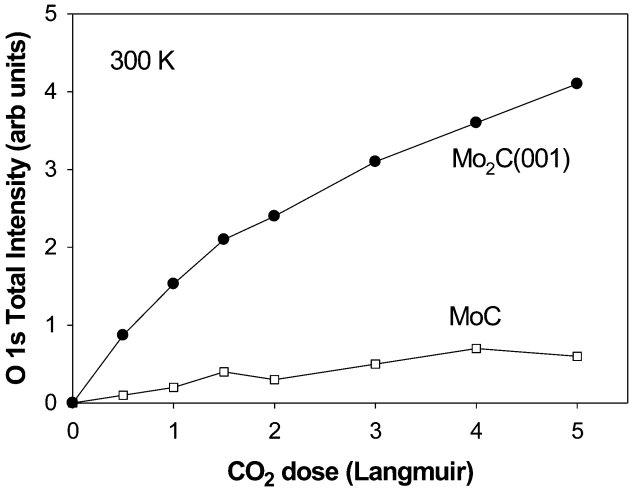

Fig. 6 Variation of the total O 1s signal after dosing CO_2 to polycrystalline MoC and a β-Mo_2C(001)-Mo surface. In the case of β-Mo_2C(001)-Mo, the adsorbed CO_2 underwent dissociation into O and CO.

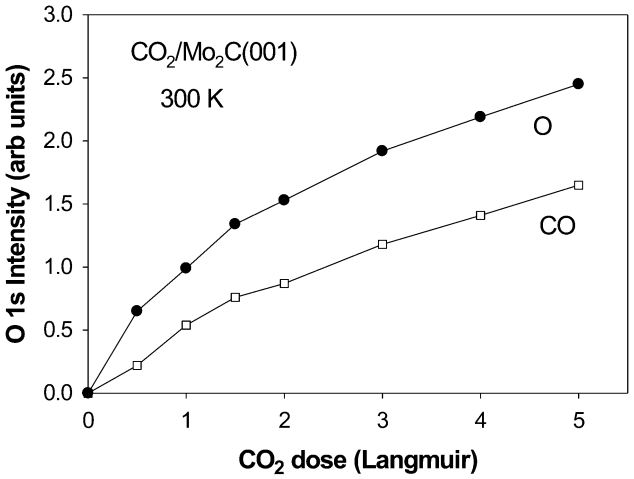

Fig. 7 Uptake of O and CO after several doses of CO_2 to β-Mo_2C(001)-Mo at 300 K.

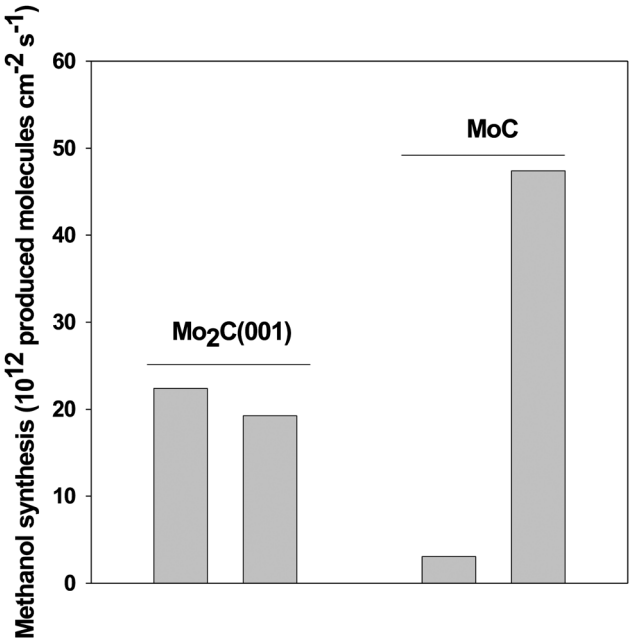

Fig. 8 Rates for the production of methanol obtained from CO_2 hydrogenation on β-Mo_2C(001)-Mo and polycrystalline MoC at 500 and 600 K. P_{CO_2} = 0.049 MPa (0.5 atm), P_{H_2} = 0.441 MPa (4.5 atm).

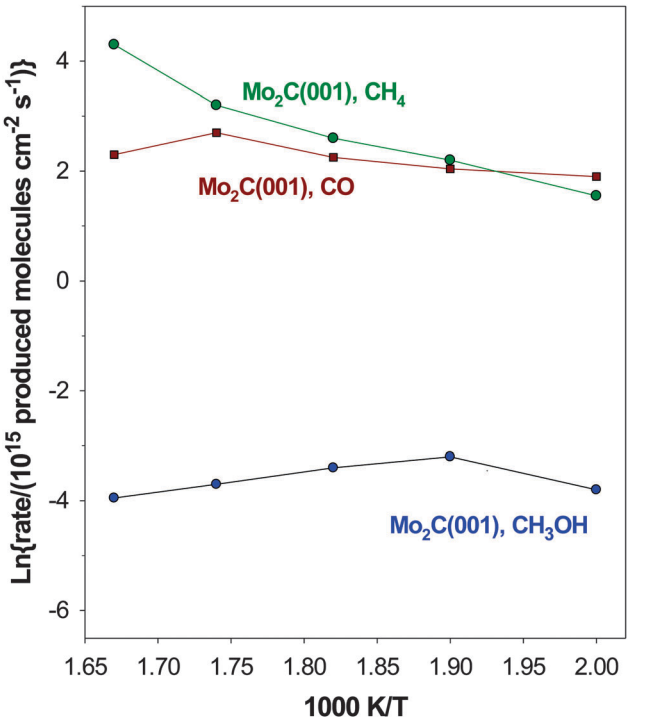

Fig. 9 Arrhenius plots for the production of CO, methane and methanol on β-Mo_2C(001)-Mo. In a batch reactor, the metal carbide catalyst was exposed to 0.049 MPa (0.5 atm) of CO_2 and 0.441 MPa (4.5 atm) of H_2 at temperatures of 600, 575, 550, 525, and 500 K.

At 600 K, the β-Mo_2C(001)-Mo substrate probably fully decomposes a large fraction of the adsorbed CO_2 molecules. Under these conditions, β-Mo_2C(001)-Mo is an excellent catalyst for methane production.

In our studies, we found that the major products of the hydrogenation of CO_2 on β-Mo_2C(001)-Mo are CO, CH_4, and CH_3OH. We also found traces of C_2H_6, CH_3OCH_3, and C_2H_5OH. Fig. 9 shows how the rate of formation of CO, CH_4, and CH_3OH changes as a function of temperature. The main products of the reaction are CO, produced through the reverse water–gas shift reaction, and methane. Temperature has a strong effect on the selectivity of the β-Mo_2C(001)-Mo catalyst. At very high temperature (> 575 K), $CO_2 \rightarrow C + 2O$ full decomposition probably takes place and one sees an enhancement in the rate of CH_4 formation and a substantial drop in the production of CO and CH_3OH.

On polycrystalline MoC, the hydrogenation of CO_2 produced only CO and CH_3OH. Fig. 10 shows Arrhenius plots for the generation of CO and methanol on MoC. MoC exhibits a catalytic activity higher than that of Cu(111),[47] a surface that is commonly used as a benchmark in catalytic studies,[46,47] and a TiC(001) catalyst.[45] From the Arrhenius plot in Fig. 10, one can estimate an apparent activation energy of 17.2 kcal mol^{-1} for the synthesis of methanol from CO_2 hydrogenation on MoC. This value is smaller than the corresponding values of 20.9 and 25.4 kcal mol^{-1} found on TiC(001) and Cu(111), respectively.[45,47] In the catalytic process the initial step of binding the CO_2 molecule is important because the sequence in the magnitude of the calculated CO_2 adsorption energies ($Cu^{47} \ll TiC^{45} < MoC$) matches well the sequence found for the catalytic activity. Furthermore, the results in Fig. 8 and 10 indicate that MoC is a

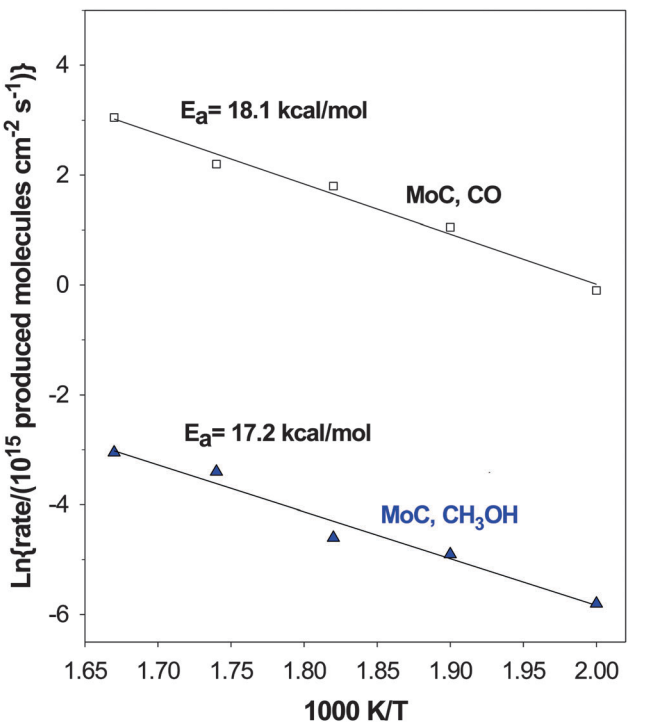

Fig. 10 Arrhenius plots for the production of CO and methanol on MoC. In a batch reactor, the metal carbide catalyst was exposed to 0.049 MPa (0.5 atm) of CO_2 and 0.441 MPa (4.5 atm) of H_2 at temperatures of 600, 575, 550, 525, and 500 K.

good and selective catalyst for methanol synthesis at high temperatures. When going from Mo_2C to MoC, the increase in the carbon content of the carbide moderates the reactivity of the Mo centers which still can bind well the CO_2 molecule but now the cleavage of the first C–O bond must be assisted by hydrogen ($H + OCO \rightarrow HOCO \rightarrow HO + CO$)[52] and there is no rupture of the second C–O bond. As a result of this property, MoC is a selective catalyst for a $CO_2 \rightarrow CH_3OH$ transformation. The theoretical results in Table 1 and the experimental data in Fig. 9 and 10 illustrate the tremendous impact that the carbon/metal ratio has on the chemical and catalytic properties of molybdenum carbides. This ratio must be taken into consideration when designing catalysts for the activation and conversion of CO_2.

Conclusions

Periodic DFT calculations and experiments on controlled conditions have been carried out to investigate CO_2 adsorption and subsequent hydrogenation on MoC and Mo_2C surfaces. The DFT calculations have been carried out using the PBE functional and explicitly accounting for a description of vdW forces. The study also addresses to determine whether there are differences in the reactivity of both β-Mo_2C(001) terminations, depending on whether the layer that interacts with the CO_2 is built up of C or Mo atoms. Results show that the vdW correction provides no structural differences in the optimized structures. Therefore, these forces are not decisive in CO_2 adsorption and activation. Furthermore, it is found that the CO_2 molecule can be activated in all the studied cases. The reactivity of the δ-MoC and β-Mo_2C(001)-C surfaces is similar, sharing a charge transfer surface $\rightarrow CO_2$ of $\sim$0.75–1 electron, leading to the formation of C–C bonds. The adsorption energy values are at the fringe of chemical interaction, regardless of the covalent C–C bond formation. These surfaces point to a posterior reaction of the activated CO_2 to form suitable products, such as methanol or formic acid *via* hydrogenation. The adsorption energy values show, however, that CO_2 adsorption is most favorable on β-Mo_2C(001)-Mo. Here a majority of CO_2 can adopt an activated chemisorbed situation, whereas a fraction of molecules may suffer a spontaneous rupture of a C–O bond leading to the formation of the CO moiety.

The predictions from the DFT calculations were confirmed by experimental tests which showed that Mo-terminated β-Mo_2C(001) easily adsorbs and decomposes the CO_2 molecule. Moreover, there is clear experimental evidence that this surface is an active catalyst for the hydrogenation of CO_2 to methanol and methane. The experiments also show that MoC binds and activates CO_2 better than transition metal surfaces and that it is an active and selective catalyst for the $CO_2 + 3H_2 \rightarrow CH_3OH + H_2O$ reaction.

The theoretical calculations also indicate that there are very large differences in reactivity between the two β-Mo_2C(001) endings and are in agreement with the experimental evidence of CO_2 breaking on the β-Mo_2C(001)-Mo terminated surface. All in all, the present results show the high activity of molybdenum carbide surfaces in CO_2 activation, surpassing even that of other transition metal carbide surfaces such as TiC(001). Moreover, the present combined theoretical and experimental study illustrates the tremendous impact that the carbon/metal ratio has on the chemical and catalytic properties of molybdenum carbide surfaces. This ratio must be taken into consideration when designing catalysts for the activation and conversion of CO_2.

Acknowledgements

The research carried out at the *Universitat de Barcelona* was supported by the Spanish MINECO grant CTQ2012-30751 grant and, in part, by *Generalitat de Catalunya* (grants 2014SGR97 and XRQTC). The research carried out at BNL was supported by the U.S. Department of Energy, Chemical Sciences Division (DE-AC02-98CH10886). S.P.P acknowledges financial support from Spanish MEC predoctoral grant associated with CTQ-2012-30751; F.V. thanks the MINECO for a postdoctoral *Juan de la Cierva* grant (JCI-2010-06372); F.I. acknowledges additional support through the ICREA Academia award for excellence in research and P.J.R. is grateful to INTEVEP and IDB for support of the work carried out at UCV. Computational time at the *MARENOSTRUM* supercomputer has been provided by the Barcelona Supercomputing Centre through a grant from *Red Española de Supercomputación*.

References

1 D. Preti, C. Resta, S. Squarcialupi and G. Fachinetti, *Angew. Chem., Int. Ed.*, 2011, **50**, 12551.
2 M. Behrens, F. Studt, I. Kasatkin, S. Kühl, M. Hävecker, F. Abild-Pedersen, S. Zander, F. Girgsdies, P. Kurr, B. L. Kniep, M. Tovar, R. W Fischer, J. K. Nørskov and R. Schlögl, *Science*, 2012, **336**, 893.
3 M. Ansari, B.-H. Min, Y.-H. Mo and S.-E. Park, *Green Chem.*, 2011, **13**, 1416.
4 *Carbon Dioxide as Chemical Feedstock*, ed. M. Aresta, Wiley-VCH, New York, 2010.
5 F. Viñes, A. Borodin, O. Höfft, V. Kempter and F. Illas, *Phys. Chem. Chem. Phys.*, 2005, **7**, 3866.
6 M. Fernández-García and J. A. Anderson, *Supported Metals in Catalysis*, Catalytic Sciences Series, Imperial College Press, London, 2005, vol. 5; A. Wieckowski, E. Savinova and C. G. Vayenas, *Catalysis and Electrocatalysis at Nanoparticle Surfaces*, Marcel Dekker, New York, 2003.
7 Chemisorption and Reactivity on Supported Clusters and Thin Films: Towards an Understanding of Microscopic Processes in Catalysis (NATO Science Series E: (closed)) by R. M. Lambert and G. Pacchioni (Dec 3, 2010).
8 J. M. Thomas and W. J. Thomas, *Principles and Practice of Heterogeneous Catalysis*, Wiley-VCH, New York, 1996.
9 L. E. Toth, *Transition Metal Carbides and Nitrides*, Academic Press, New York, 1971.
10 F. Viñes, C. Sousa, P. Liu, J. A. Rodriguez and F. Illas, *J. Chem. Phys.*, 2005, **122**, 174709.
11 R. B. Levy and M. Boudart, *Science*, 1973, **181**, 547.

12 J. A. Rodriguez, P. Liu, F. Viñes, F. Illas, Y. Takahashi and K. Nakamura, *Angew. Chem., Int. Ed.*, 2008, **47**, 6685.
13 J. A. Rodriguez, P. Liu, Y. Takahashi, K. Nakamura, F. Viñes and F. Illas, *J. Am. Chem. Soc.*, 2009, **131**, 8595.
14 L. Feria, J. A. Rodriguez, T. Jirsak and F. Illas, *J. Catal.*, 2011, **279**, 352.
15 J. A. Rodriguez, P. Liu, Y. Takahashi, K. Nakamura, F. Viñes and F. Illas, *Top. Catal.*, 2010, **53**, 393.
16 J. A. Rodriguez, P. Liu, Y. Takahashi, F. Viñes, L. Feria, E. Florez, K. Nakamura and F. Illas, *Catal. Today*, 2011, **166**, 2.
17 J. A. Rodriguez, L. Feria, T. Jirsak, Y. Takahashi, K. Nakamura and F. Illas, *J. Am. Chem. Soc.*, 2010, **132**, 3177.
18 E. Florez, T. Gomez, P. Liu, J. A. Rodriguez and F. Illas, *ChemCatChem*, 2010, **2**, 1219.
19 L. K. Ono and B. Roldán-Cuenya, *Catal. Lett.*, 2007, **113**, 86.
20 G. G. Asara, L. Feria, E. Florez, J. M. Ricart, P. Liu, J. A. Rodriguez and F. Illas, *J. Phys. Chem. C*, 2011, **1115**, 22495.
21 F. Viñes, J. A. Rodriguez, P. Liu and F. Illas, *J. Catal.*, 2008, **260**, 103.
22 P. Liu and J. A. Rodriguez, *J. Phys. Chem. B*, 2006, **110**, 19418.
23 N. M. Schweitzer, J. A. Schaidle, O. K. Ezekoye, X. Pan, S. Linic and L. T. Thompson, *J. Am. Chem. Soc.*, 2011, **133**, 2378.
24 J. Ren, C.-F. Huo, J. Wang, Z. Cao, Y.-W. Li and H. Jiao, *Surf. Sci.*, 2006, **600**, 2329.
25 H. Tominaga and M. Nagai, *Appl. Catal., A*, 2007, **328**, 35.
26 A. J. Medford, A. Vojvodic, F. Studt, F. Abild-Pedersen and J. K. Nørskov, *J. Catal.*, 2012, **290**, 108.
27 F. Viñes, C. Sousa, F. Illas, P. Liu and J. A. Rodriguez, *J. Phys. Chem. C*, 2007, **111**, 16982.
28 W. Zheng, T. P. Cotter, P. Kaghazchi, T. Jacob, B. Frank, K. Schlichte, W. Zhang, D. S. Su, F. Schüth and R. Schlögl, *J. Am. Chem. Soc.*, 2013, **135**, 3458.
29 H. Tominaga, Y. Aoki and M. Nagai, *Appl. Catal., A*, 2012, **423–424**, 192.
30 C. Pistonesi, M. E. Pronsato, L. Bugyi and A. Juan, *J. Phys. Chem. C*, 2012, **116**, 24573.
31 J. W. Han, L. Li and D. S. Scholl, *J. Phys. Chem. C*, 2011, **115**, 6870.
32 T. Wang, Y. W. Li, J. Wang, M. Beller and H. Jiao, *J. Phys. Chem. C*, 2014, **118**, 3162.
33 G. Kresse and J. Furthmüller, *Phys. Rev. B: Condens. Matter Mater. Phys.*, 1996, **54**, 11169.
34 J. P. Perdew, K. Burke and M. Ernzerhof, *Phys. Rev. Lett.*, 1996, **77**, 3865.
35 J. R. d. S. Politi, F. Viñes, J. A. Rodriguez and F. Illas, *Phys. Chem. Chem. Phys.*, 2013, **15**, 12617.
36 S. Grimme, *J. Comput. Chem.*, 2006, **27**, 1787.
37 P. E. Blöchl, *Phys. Rev. B: Condens. Matter Mater. Phys.*, 1994, **50**, 17953.
38 G. Kresse and D. Joubert, *Phys. Rev. B: Condens. Matter Mater. Phys.*, 1999, **59**, 1758.
39 F. Viñes, C. Sousa, F. Illas, P. Liu and J. A. Rodriguez, *J. Phys. Chem. C*, 2006, **111**, 1307.
40 F. Viñes, A. Vojvodic, F. Abild-Pedersen and F. Illas, *J. Phys. Chem. C*, 2013, **117**, 4168.
41 H. J. Monkhorst and J. D. Pack, *Phys. Rev. B: Solid State*, 1976, **13**, 5188.
42 P. Liu, J. A. Rodriguez, T. Asakura, J. Gomes and K. Nakamura, *J. Phys. Chem. B*, 2005, **109**, 4575.
43 T. P. Saint Clair, S. T. Oyama, D. F. Cox, S. Otani, Y. Ishizawa, R. L. Low, K. Fukui and Y. Iwasawa, *Surf. Sci.*, 1999, **426**, 187.
44 J. G. Chen, *Chem. Rev.*, 1996, **96**, 1447.
45 A. B. Vidal, L. Feria, J. Evans, Y. Takahashi, P. Liu, K. Nakamura, F. Illas and J. A. Rodriguez, *J. Phys. Chem. Lett.*, 2012, **3**, 2275.
46 J. Yoshihara and C. T. Campbell, *J. Catal.*, 1996, **161**, 776.
47 Y. Yang, J. Evans, J. A. Rodriguez, M. G. White and P. Liu, *Phys. Chem. Chem. Phys.*, 2010, **12**, 9909.
48 S. Y. Wu and J. J. Ho, *J. Phys. Chem. C*, 2012, **116**, 13202.
49 R. F. Bader, *Atoms in Molecules: A Quantum Theory*, Oxford Science, Oxford, U.K., 1990.
50 L. Bugyi, A. Oszko and F. Solymosi, *Surf. Sci.*, 2000, **461**, 177.
51 T. P. Saint Clair, S. T. Oyama and D. F. Cox, *Surf. Sci.*, 2000, **468**, 62.
52 J. A. Rodriguez, J. Evans, L. Feria, A. B. Vidal, P. Liu, K. Nakamura and F. Illas, *J. Catal.*, 2013, **307**, 162.